INTERNATIONAL DESIGN CONFERENCE - DESIGN 2002
Dubrovnik, May 14 - 17, 2002.

NUMERICAL SIMULATION OF MICRO-PITTING ON GEARS

G. Fajdiga, J. Flašker and S. Glodež

Keywords: Contact mechanics, EHD Lubrication, Numerical Fracture Mechanics, Micro Pitting

1. Introduction

The pitting of gear teeth flanks is characterised by occurrence of small pits on the contact surfaces. Pitting originates from small, surface or subsurface initial cracks, which grow under repeated contact loading. At some point the cracks curve back towards the surface, which eventually causes the material surface layer to break away and a void occurs on the surface. Although surface pitting is a well-known problem in engineering and many hypotheses and models have been proposed to-date, the general theory to realistically describe the complicated mechanism completely has yet to be established. Some early attempts to apply fracture mechanics to the study of pit formation mechanisms [Zhou 1989], led to some very comprehensive computational models to be proposed more recently [Murakami 1994, Glodež 1997, Fajdiga 2001]. These models assume that the crack is initiated on or under the surface due to significant friction forces or as a consequence of mechanical and thermal treatment of the material. Under cyclic contact loading the crack then propagates from the initial to the critical crack length, when a pit is formed on the surface. This paper describes a computational model, which attempts to account for different parameters influencing the pitting process (Hertzian contact pressure, friction between contacting surfaces, EHD-lubrication, moving contact of gear flanks, fluid trapped in the crack).

2. Parameters influencing the fatigue crack growth

2.1 Normal and tangential contact loading

The normal contact pressure between meshing gear flanks has been determined using the Hertzian theory [Johnson 1985], where the distribution of normal contact pressure $p(x)$ can be analytically determined by (see Figure 1)

$$p(x) = \frac{2F_N}{\pi b^2}\sqrt{b^2 - x^2}, \tag{1}$$

where F_N is the normal force per unit gear width and b is the half-length of the contact area, which can be determined from

$$b = \sqrt{\frac{8F_N R^*}{\pi E^*}}, \tag{2}$$

where R^* and E^* are the equivalent radius and the equivalent Young's modulus, respectively, defined as

$$R^* = \frac{R_1 \cdot R_2}{R_1 + R_2}, \tag{3}$$

$$E^* = \frac{2E_1E_2}{E_2(1-\nu_1^2) + E_1(1-\nu_2^2)}, \tag{4}$$

where R_1, E_1, ν_1 and R_2, E_2, ν_2 are the curvature radii, Young's modulus and Poisons ratio of contacting cylinders, see Figure 1a.

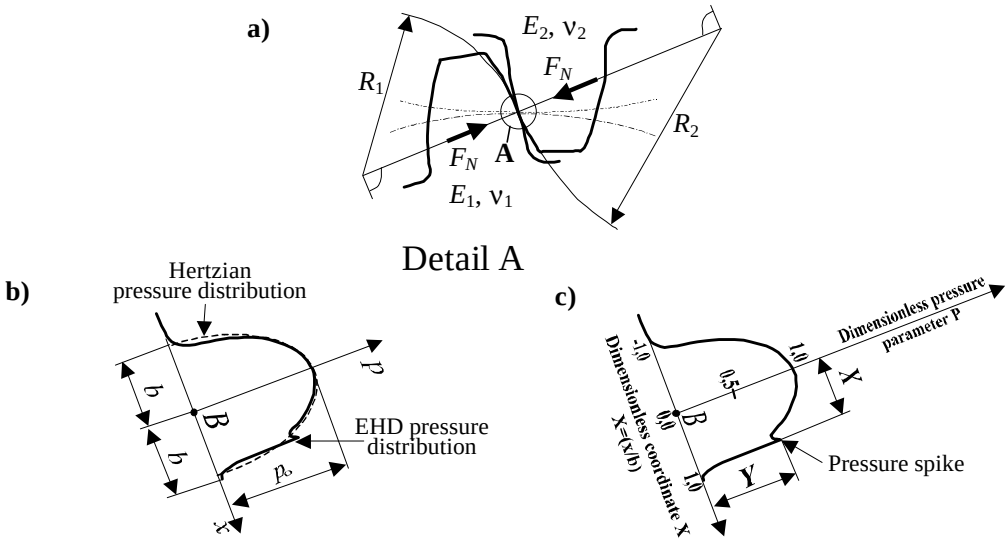

Figure 1. Loading conditions in the contact area of gear teeth flanks

The maximum contact pressure $p_0=p(x=0)$ can then easily be determined as

$$p_0 = \sqrt{\frac{F_N \cdot E^*}{2\pi R^*}} \cdot \tag{5}$$

The distribution of tangential contact loading $q(x)$ due to the relative sliding of gear flanks is here determined by utilising the Coulomb friction law

$$q(x) = \mu \cdot p(x), \tag{6}$$

where μ is the coefficient of friction between meshing gear flanks.

2.2 Influence of the EHD-lubrication

In the proposed computational model the normal contact loading distribution $p(x)$ considers also the influence of the elasto-hydro-dynamic (EHD) lubrication conditions, which appear in the contact of lubricated gear flanks. Under such conditions, the contacting surfaces are separated with a thin lubricant film. However, the presence of the viscous lubricant in the contact area of sliding surfaces affects the contact pressure distribution in a way that is illustrated in Figure 1b. This pressure distribution can be determined experimentally or with the use of appropriate computational models [Dowson 1977]. A significant pressure spike develops in the outlet contact region and strongly depends on the lubricant's pressure-viscosity characteristic [Dowson 1977]. In computations reported herein the dimensionless pressure spike amplitude Y and dimensionless pressure spike location X (see Figure 1c) have been determined using following empirical equations [Hamrock 1987]:

$$Y = 0.267\, W^{-0.375} U^{0.174} G^{0.219} \tag{7}$$

$$X = 1 - 2.469\, W^{-0.941} U^{0.206} G^{-0.848} \tag{8}$$

where *W*, *U* and *G* are dimensionless parameters [Hamrock 1987] .

2.3 Influence of moving contact and lubricant trapped in the crack

For more realistic simulation of the fatigue crack growth it is necessary to consider the moving contact of gear flanks. The moving contact can be simulated with different loading configurations as it is shown on Figure 2a. In all configurations the normal $p(x)$ and tangential $q(x)$ contact loading distributions are of the same magnitude, however they are acting at different positions in respect to the crack.

The simulation of the surface initiated fatigue crack propagation needs to consider also the influence of the lubricant pressure acting on the crack faces. The lubricant pressure is not constant and is dependent on the contact loading position, *i.e.* the contact pressure distribution position in respect to the crack, see Figure 2b. When the contact loading p_1 is acting over the crack (position 1), the crack faces are also loaded with the lubricant pressure p_1. In position 2 the crack faces are loaded with the lubricant pressure p_2. Following this the appropriate lubricant pressure can be determined for all load cases considered in Figure 2a.

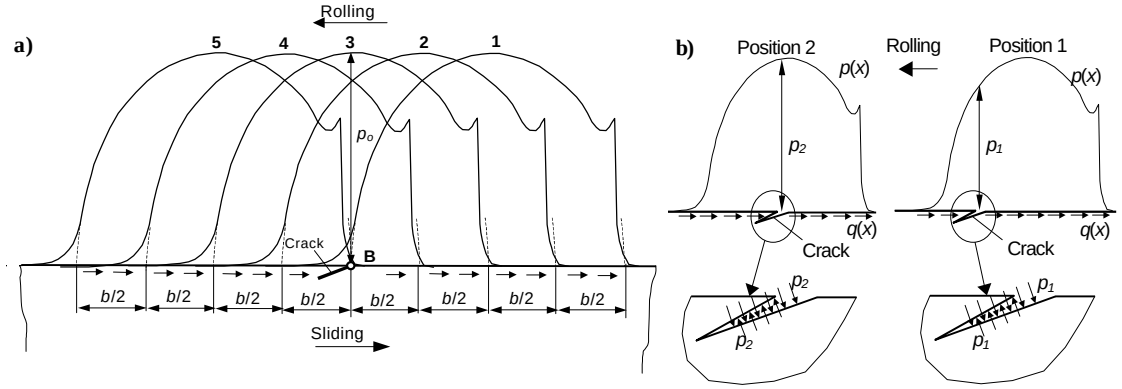

Figure 2. Moving contact loading configurations (a) and crack face loading with the lubricant pressure (b)

2.4 Fatigue crack propagation under contact loading

For the purpose of the fatigue crack growth simulation, the virtual crack extension (VCE) method in the framework of the finite element method (FEM) has been applied. The VCE-Method, originally proposed by Hellen [Hellen 1975], is based on the criteria of released strain energy d*V* per crack extension d*a*

$$G = -\frac{\mathrm{d}V}{\mathrm{d}a} \tag{9}$$

where *G* is the energy release rate, which serves as a basis for determination of the combined stress intensity factor *K* around the crack tip for plain strain conditions

$$K = \sqrt{\frac{E \cdot G}{(1-\nu^2)}} \tag{10}$$

where *E* is the Young's modulus of the material and ν is the Poison ratio. The combined stress intensity factor *K* is for 2D problems determined as follows:

$$K = \sqrt{(K_I^2 + K_{II}^2) \cdot (1-\nu^2)} \tag{11}$$

where K_I and K_{II} are the stress intensity factors for mode I and II of crack growth. The complete procedure for determination of the combined stress intensity factor K using VCE-Method is fully described in [Hellen 1975].
Assuming the validity of the maximum energy release criterion, the crack will propagate in that direction corresponding to the maximum value of G, *i.e.* in the direction of the maximum stress intensity factor K. The computational procedure is based on incremental crack extensions, where the size of the crack increment is prescribed in advance. The virtual crack increment should not exceed 1/3 of the size of crack tip finite elements. For each crack extension increment, the stress intensity factor is determined in several different possible crack propagation directions (Figure 3a) and the crack is actually extended in the direction of the maximum stress intensity factor, which requires local remeshing around the new crack tip.

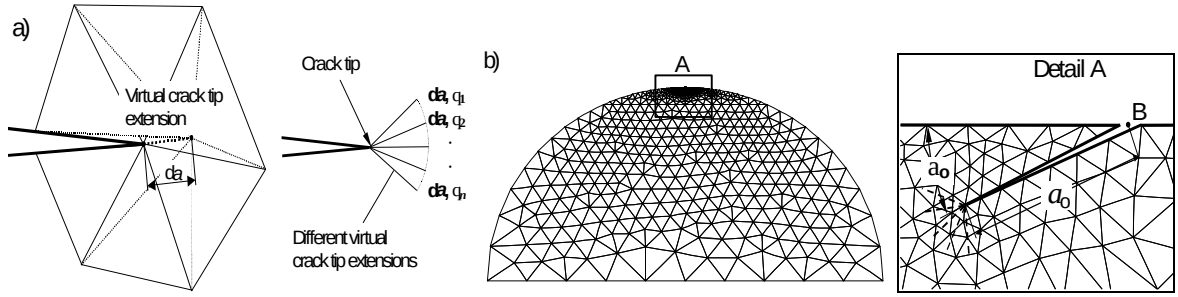

Figure 3. Virtual crack tip extension technique (a) and FE discretisation (b)

The incremental procedure is repeated until crack tip reaches the vicinity of contact surface, when surface pit can be expected to occur, see Figure 5. For improved numerical results, special fracture finite elements are used in the first circle of elements around a crack tip. Following the above procedure, one can numerically determine the functional relationship $K=f(a)$.

3. Practical applications

The proposed computational model has been applied for analyses of the surface initiated fatigue crack growth using the equivalent contact model and influencing parameters described in former section. The numerical simulations have been done for various combinations of contacting surface curvatures and loadings: R^*=6, 8, 10, 14, 20 mm and p_0=1000, 1550, 1700 N/mm^2. For all computations, Young's modulus $E=2.06\cdot10^5$ N/mm^2, Poisson ratio ν=0.3 and the coefficient of friction μ=0.04, which is the average value for well-lubricated mechanical elements [Winter 1990], have been used. The EHD-pressure distribution in the contact zone has been estimated using eqs. (7) and (8) for the lubricant oil ISO-VG-100 with the kinematic viscosity ν_{40} = 100 mm^2/s, density ρ_{15} = 0.877 kg/dm^3 and pressure-viscosity coefficient $\alpha=0.15\cdot10^{-7}$ m^2/N. The mean surface velocity of the contacting surfaces has been taken as a constant value u=6 m/s, which is a commonly used value for gears [Winter 1990]. Using these parameters the dimensionless pressure spike amplitude Y and dimensionless pressure spike location X (see Figure 1c) have been determined for all combinations of p_0 and R^* as described above. The calculated pressure spike has been in numerical computations considered as the additional nodal force along distribution of contact pressure p(x). The finite element mesh, shown in Figure 3b, and normal and tangential loading as described above have been used in the subsequent analyses. For the configuration of the initial crack on the surface, located at point B, it was assumed that the initial length of the crack is equal to a_o=15 μm with the initial inclination angle towards the contact surface equal to α_o = 22°. This configuration follows the metallographic investigations of initial cracks appearing on the contacting mechanical elements of gears and bearings [Elstorpff 1993]. In this study, the FE analysis program BERSAFE [Bersafe 1988] has been used for computational estimation of the stress intensity factor K and subsequent incremental crack growth simulation. In all computations the crack increment was of size Δa = 1.5 μm. The stress intensity factor K was estimated in each crack increment for 30 different virtual crack tip extensions (see Figure 3a). Five different loading configurations have been considered in each computation for the purpose of simulating the effect of

the moving contact of the mechanical elements (see Figure 2a). For each crack increment the crack was actually extended in the direction of the recorded K_{max} of all calculated load cases. In Figure 4, the relationship between stress intensity factor K and crack length a is shown for different values of the equivalent radius R^* and maximum contact pressure p_0. In the first two calculation steps, the maximum stress intensity factor K_{max} appears under the load case 5 (see Figure 4), while later load case 3 dominates. Figure 4 illustrate that the computed stress intensity factor K is very small at the beginning but later increases as the crack propagates towards the contact surface. Numerical simulations have shown that at the moment when the crack reaches the vicinity of the contact surface, the stress intensity factor is extremely high. At that moment it can be expected that the material surface layer breaks away and the pit occurs on the surface. Because of very small dimensions of surface pits, they can be termed as micro-pitting.

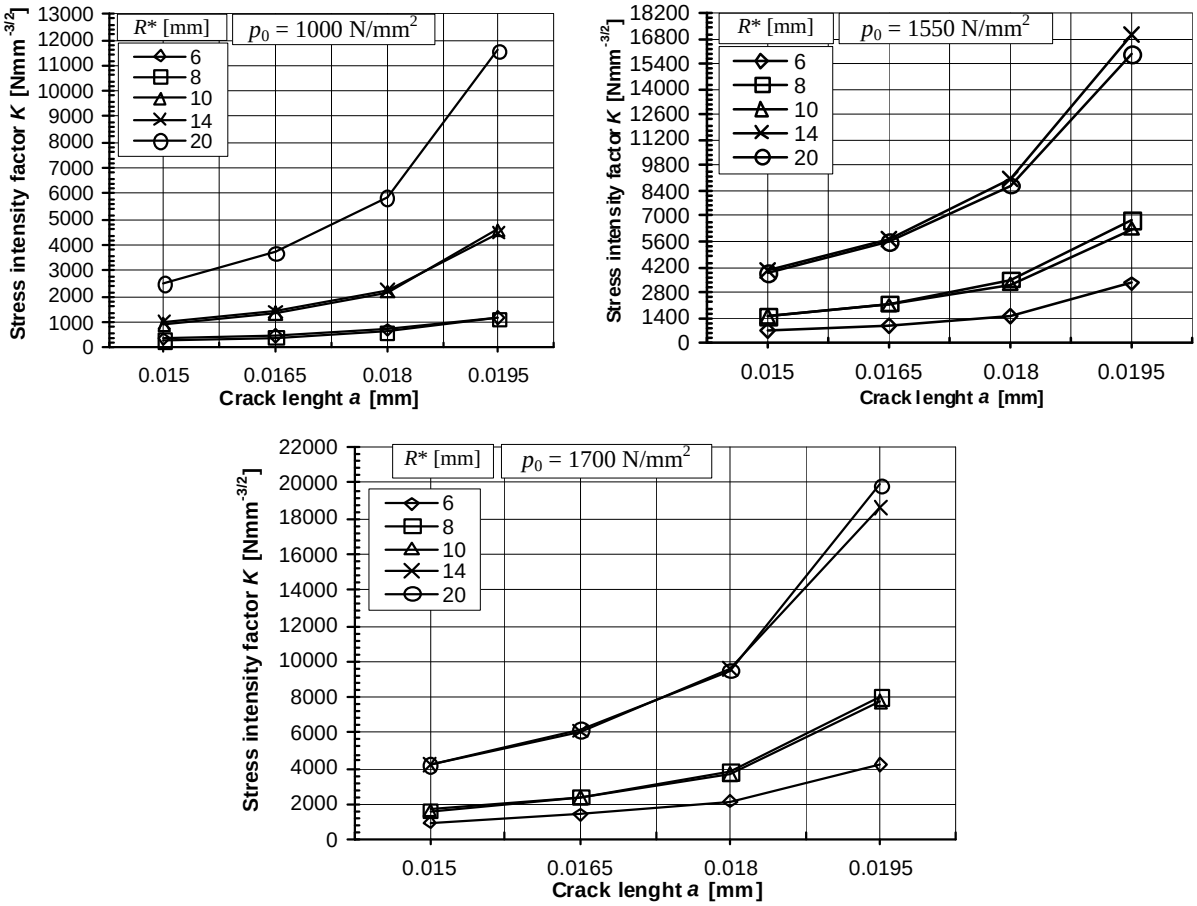

Figure 4. Stress intensity factor *K* for different maximum contact pressures

Figure 5 shows that the shape and magnitude of numerically determined pits correspond well with available experimental data [Elstorpff 1993], which have been determined with experimental testing of the spur gear pair using FZG- pitting test machine according to DIN 51354 standard.

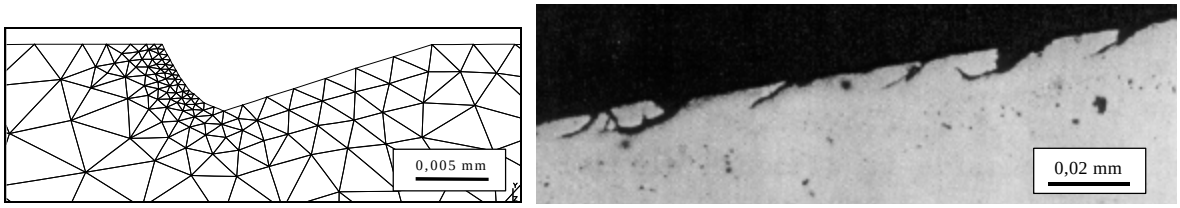

Figure 5. Numerically (a) and experimentally (b) determined pit shapes

4. Concluding remarks

The paper presents a computational model for the simulation of surface initiated fatigue crack growth on contacting mechanical elements as used in gears, bearings, wheels, etc. A simple equivalent model of two cylinders is used for simulation of fatigue crack growth under conditions of rolling and sliding contact. The equivalent model is subjected to the normal (normal contact pressure) and tangential (frictional forces) contact forces which also take into account the influence of EHD-lubrication conditions as well as the associated lubricant pressure acting on the crack faces. The virtual crack extension method in the framework of finite element analysis is used for simulating the fatigue crack propagation from the initial crack up to the formation of the surface pit. The pit shapes and relationships between the stress intensity factor and crack length are determined for various combinations of contacting surface curvatures and loadings. On the basis of the results in Figures 4 and 5, it can be concluded that the initial surface crack of length 15 μm with the considered boundary conditions lead to the appearance of very small surface pits, which can be termed as micro-pitting on the contacting mechanical elements. The numerical results correspond well with available experimental data. Consequent computational determination of the functional relationship $K = f(a)$ from diagrams on Figure 4 enables estimation of the service life of contacting mechanical elements in regard to the surface pitting, if combined with previously developed model [Glodež 1997, Fajdiga 2001]. The small crack lengths imply that the short crack growth theory should be used for the description of fatigue crack propagation as described in above mentioned references. However, the model can be further improved with additional theoretical, numerical and foremost experimental research, since it relies mostly on experimentally determined material parameters.

References

Zhou R. S., Cheng H. S. and Mura T., "Micropitting in Rolling and sliding contact under mixed lubrication", ASME J. Tribology, 111, pp. 605-613, 1989.

Murakami Y., Sakae C, Ichimaru K., "Three-dimensional fracture mechanics analysis of pit formation mechanism under lubricated rolling-sliding contact loading", STLE Trib. Trans., 37, pp. 445-454, 1994.

Glodež S., Winter H., Stüwe H.P., "A fracture mechanics model for the wear of gear flanks by pitting", Wear, 208, pp. 177-183, 1997.

Fajdiga G. Flašker J., Glodež S. and Hellen T., "Numerical modelling of surface pitting of gear teeth flanks", Int. j. Fatigue & Fracture of Eng. Mat. & Struct., in publication, 2001.

Johnson K. L., "Contact mechanics", Cambridge University press, 1985.

Dowson D., "Elasto-hydrodynamic lubrication", Pergamon Press, 1977.

Hamrock B.J., Lee R.T., Houpert L.G., "Parametric study of performance in elastohydrodynamic lubricated line contact", Fluid film lubrication–Osborne Reynolds centenary, pp. 199-206, 1987.

Hellen T. K., "On the method of virtual crack extensions", International Journal for Numerical Methods in Engineering, 9, pp. 187-207, 1975.

Winter H., Knauer G.,"Einfluss von Schmierstoff und Betriebstemperatur auf die Grübchentragfähigkeit einsatzgehärteter Zahnräder", Antriebstechnik, 29, pp. 65-84, 1990.

BERSAFE, Users's Guides, Vol. 2, 1988

Elstorpff Marc-G.,"Einflüsse auf die Grübchentragfähigkeit", Ph.D., thesis, TU Munich, 1993.

Gorazd Fajdiga, Univ. Dipl. Ing., M. Sc., Ph.D.
University of Maribor
Faculty of Mechanical Engineering
Laboratory for computer aided engineering
Smetanova street 17, 2000 Maribor
SLOVENIA
Telephone: (386) 62 220 7708
Fax: (386) 62 220 7990
Email: gorazd.fajdiga@uni-mb.si